COBEM 2023 27TH INTERNATIONAL CONGRESS OF MECHANICAL ENGENEERING

ABCM Brazilian Society of Mechanical Sciences and Engineering
27th ABCM International Congress of Mechanical Engineering
December 04-08, 2023, Florianópolis-SC, Brazil

# COB-2023-1623
# DESIGN OF A SMALL-CAPACITY REFRIGERATION MACHINE OPERATING WITH R744 AND CAPILLARY TUBE

**Willian Moreira Duarte**
Federal University of Minas Gerais (UFMG), Graduate Program in Mechanical Engineering (PPGMEC)
Av. Pres. Antônio Carlos, 6627 - Pampulha, Belo Horizonte - MG, 31270-901, Brazil.
willian@demec.ufmg.br

**Lucas Cordeiro Pereira Lima**
**Yuri Figueiredo de Paula**
Federal University of Minas Gerais (UFMG), Undergraduate Program in Mechanical Engineering
Av. Pres. Antônio Carlos, 6627 - Pampulha, Belo Horizonte - MG, 31270-901, Brazil.
cordeirolucas161@ufmg.br,yuri03@ufmg.br

**Tiago de Freitas Paulino**
Federal Center of Technological Education of Minas Gerais (CEFET-MG), Graduate Program in Mechanical Engineering
Av. Amazonas, 5253 - Nova Suiça, Belo Horizonte - MG, 30421-169, Brazil
tfpaulinoeng@gmail.com

**Antônio Augusto Torres Maia**
Federal University of Minas Gerais (UFMG), Graduate Program in Mechanical Engineering (PPGMEC)
Av. Pres. Antônio Carlos, 6627 - Pampulha, Belo Horizonte - MG, 31270-901, Brazil.
aamaia@demec.ufmg.br

***Abstract.*** *The refrigeration industry has been moving towards environmentally friendly refrigerants, and R744 (carbon dioxide) is a potential solution. The use of R744 as a refrigerant has been gaining attention due to its low environmental impact, non-toxic nature, and favorable thermodynamic properties. Despite these advantages, manufacturing small-capacity refrigeration systems operating with R744 has become increasingly less common, probably due to the higher operating pressures compared to other refrigerants, which require specialized components and materials that can withstand high pressures. In addition, the design of these systems can also be challenging due to the selection of the most appropriate correlations to design the heat exchangers and the need to match the design requirements with the parts available on the market for assembling the system. This work aims to present a set of guidelines for designing a small-capacity refrigeration machine operating with R744. The machine has a cooling capacity of 600 W to 1200 W, and operates with an evaporating temperature from 0 to 15°C and a gas cooler pressure from 80 to 105 bars. For the reference condition, the length of the evaporator estimated was 12.9m, the length of the gas cooler was 20.6m and the cooling capacity was 855W.*

***Keywords:*** *Small-Capacity Refrigeration Machine, R744, CO2, Transcritical Operation, Ecological fluid.*

## 1. INTRODUCTION

The refrigeration equipment industry has invested in the development of systems that operate with environmentally friendly fluids, which have a low impact on global warming and are harmless to the ozone layer. This behavior is part of the efforts that companies have made to meet the commitments established in the Kyoto Protocol and the Kigali Amendment. The former sets deadlines for the reduction of greenhouse gas emissions and the latter sets deadlines for phasing out the use of hydrofluorocarbons (HFCs) (de Paula *et al.*, 2020a).

In addition to being ozone-friendly and having low Global Warming Impact (GWP), the refrigerants under consideration must have favorable thermodynamic characteristics that allow the system to operate with efficiency equal to or higher than current systems. In this context, the refrigerant R744 not only meets these requirements but also stands out for being a gas naturally present in the atmosphere and for not having toxic or flammable characteristics, which makes it safe to be used in refrigeration and air conditioning systems. Additionally, R744 has thermodynamic characteristics that allow it to achieve a high coefficient of performance. With proper design, R744 can provide energy-efficient operation when used in refrigeration systems.

R744 has been used for some time in commercial and industrial refrigeration systems. However, its use in small-

capacity refrigeration systems, such as those used in homes, is becoming less common. Some characteristics of R744 make it less attractive to be used in small systems. One of these is the high working pressure that requires high resistance components specially designed to operate at high pressures. These include compressors, expansion devices, and heat exchangers adapted to handle the particular characteristics of R744 as a working fluid. The availability of specific components may be limited for small equipment, and the minor variety of parts available on the market can make the design of these systems difficult.

The design of small refrigeration systems operating with R744 can be challenging. The selection of the most appropriate correlations for the heat exchanger design and the need to combine the design requirements with the diminished quantity of parts available in the market for the system construction can make the development of the project complicated. A list of new correlations to calculate the convective heat transfer coefficient for R744 in the supercritical state can be found in Cabeza *et al.* (2017), and most of these correlations require as input parameter the wall temperature. The use of computational tools to generate operation maps as a function of the characteristics of each component of the refrigeration system can be advantageous and facilitate the compatibility of the available parts with the design requirements.

The use of mathematical models for the design of vapor compression refrigeration systems has already been performed for the optimal design of refrigeration systems (de Paula *et al.*, 2020b), for the comparative study of different refrigerants when used in a heat pump (Rabelo *et al.*, 2019), for the study of the dynamic response of static evaporators in heat pumps operating with R744 (de Freitas Paulino *et al.*, 2019), for the development of multivariable controllers for refrigeration systems (Maia *et al.*, 2013). Although these mathematical models can be used in the design process of refrigeration machines, their outcomes are typically a single specification for each component, which may not be sufficient to choose among the parts available in the market. In addition, the conception of these mathematical models is usually more elaborated and is formulated to investigate more complex phenomena, often irrelevant when the main purpose is to design a classical refrigeration machine. The approach to be used in the design of refrigeration systems can be simpler but must provide operational maps that allow the designer to match the design requirements with the components available on the market. In this context, the objective of this work is to present a methodology for the design of small refrigeration systems operating with R744. All correlations and considerations used in the design of heat exchangers and expansion devices will be presented. Finally, these relations will be used to develop a computer code to generate the system operating curves for different capacities and their impact on the sizing of each system component.

## 2. METHODOLOGY

Figure 1 shows the scheme of the refrigeration system desired. The system consists of a closed-loop water evaporator connected to a reservoir containing an electric heater and an open-loop water-cooled gas cooler. The system will also have a compressor and three expansion devices: An electronic valve, a capillary tube, and a manual valve. The focus of this work is the design of heat the exchangers and the capillary tube that are not sold commercially in the international market for the cooling capacity required.

The design process of the refrigeration system starts with the specification of the water temperature at the inlet of the gas cooler and the heat exchanger pinch. The temperature at the outlet of the gas cooler is given by Eq.1:

$$T_3 = T_{wi} + \Delta T_{hx} \tag{1}$$

where $T_3$ is the refrigerant temperature at the outlet of the gas cooler, $T_{wi}$ is the water temperature at the inlet of the gas cooler, and $\Delta T_{hx}$ is the heat exchange pinch. Next, the pressure of the gas cooler is evaluated using the Yang *et al.* (2015) correlation for a maximum COP (Eq. 2):

$$P_{gc} = 2.918T_3 + 0.471T_4 - 0.018T_4T_3 - 13.955 \tag{2}$$

where $T_4$ is the temperature at the inlet of the evaporator. In Equation 2 , the pressure is calculated in bar, and the temperatures must be provided in $^o$C. The temperature at the inlet and the outlet of the evaporator is calculated by Eq. 3 and Eq. 4, respectively:

$$T_4 = T_{wo} - \Delta T_{hx} \tag{3}$$

$$T_1 = T_4 + \Delta T_{sh} \tag{4}$$

where $T_1$ and $T_{wo}$ is the R744 and water temperatures at the outlet of the evaporator and $\Delta T_{sh}$ is the superheating of the refrigerant. The mass flow rate of R744 is imposed by the compressor and can be given by Eq. 5 :

$$\dot{m}_r = N\rho_1 \forall \eta_{vol} \tag{5}$$

where $N$, $\rho_1$, $\forall$, $\eta_{vol}$ are the rotation speed, the refrigerant density at the inlet of the compressor, the compressor swept volume, and volumetric efficiency, respectively. The thermodynamic and transport properties were calculated using the

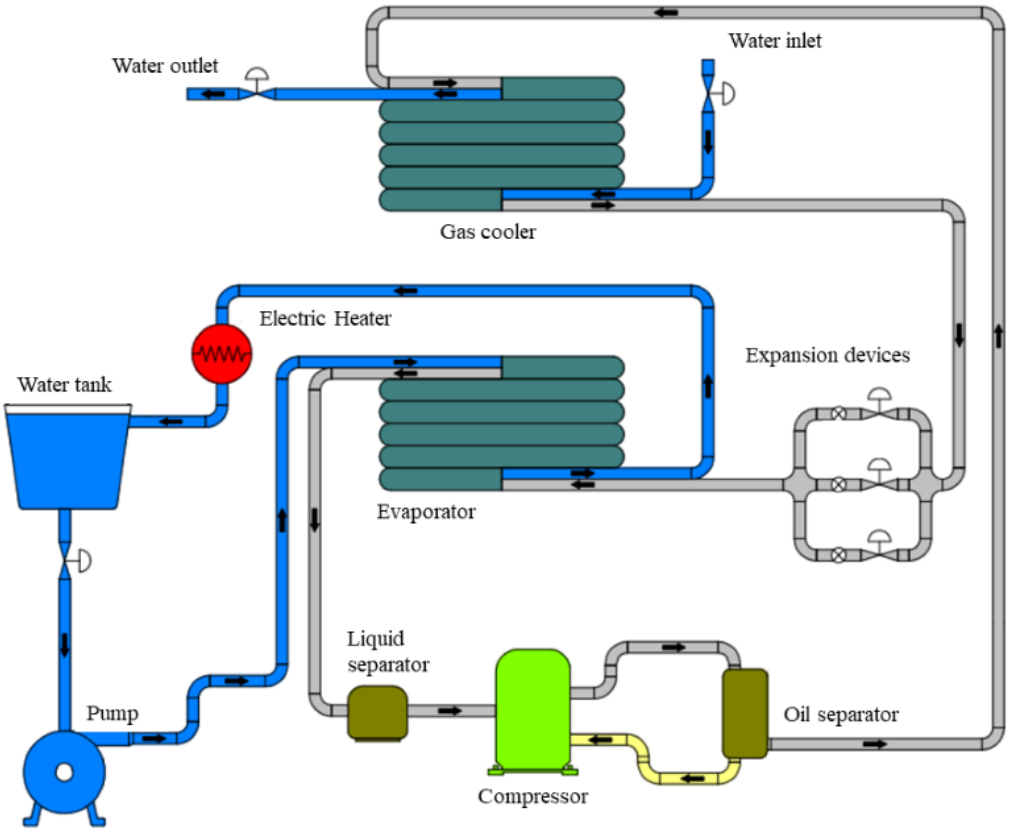


Figure 1. Schematic diagram of refrigeration machine (de Paula, 2022)

CoolProp library (Bell *et al.*, 2014). The volumetric efficiency, global efficiency ($\eta_g$), compressor swept volume, and polytropic index ($n_{pol}$) of the compressor were obtained from the experimental results presented by Humia (2022). The power consumption of the compressor is given by Eq. 6 (Humia, 2022):

$$\dot{W} = \dot{m}_r \frac{P_{gc}/\rho_2 - P_e/\rho_1}{(n_{pol} - 1)\eta_g} \tag{6}$$

The cooling capacity is given by Eq. 7:

$$\dot{Q}_e = \dot{m}_r(i_1 - i_4) \tag{7}$$

where $i$ is the specific enthalpy. The expansion process is assumed to be isenthalpic, so $i_3 = i_4$ and two independent properties are known at state 3. The mass flow rate of water in the evaporator is given by Eq. 8:

$$\dot{m}_w = \frac{c_w(T_{wi} - T_{wo})}{\dot{Q}} \tag{8}$$

where $T_{wi}$ is the water temperature at the inlet of the evaporator, $T_{wo}$ is the water temperature at the outlet of the evaporator, and $c$ is the specific heat at constant pressure, respectively. The mass flow rate is used to evaluate the Reynolds number given by Eq. 9:

$$Re = \frac{4\dot{m}}{\pi D_h \mu} \tag{9}$$

where $\mu$ and $D_h$ are dynamic viscosity and hydraulic diameter, respectively. Since the water flows in the annular space, the hydraulic diameter is the difference between the outer diameter of the inner tube ($D_{oi}$) and the inner diameter of the outer tube ($D_{io}$). If the flow is turbulent ($Re \geq 10^4$) the water heat transfer coefficient ($h_w$) is calculated using the

correlations by Gnielinski (1976) and Zigrang and Sylvester (1982), Eq. 10 and 11, respectively.

$$Nu = \frac{(f/8)(Re - 1000)Pr}{1 + 12.7(f/8)^{1/2}\left(Pr^{2/3} - 1\right)} \tag{10}$$

$$\frac{1}{\sqrt{f}} = -4\log_{10}\left[\frac{\epsilon}{3.7D_h} - \frac{5.02}{Re}\log_{10}\left(\frac{\epsilon}{3.7D_h} + \frac{13}{Re}\right)\right] \tag{11}$$

In these equations, $Nu$, $f$, $Pr$, $\epsilon$ represents the Nusselt number, the Prandtl number, the Darcy friction factor, and the rugosity, respectively. For laminar flow, the Nusselt number is interpolated from Tab. 1 where subscripts *i* and *o* represents the inner and the outer surface of the annular region.

Table 1. Nusselt number for fully developed laminar flow in annular regions (Rohsenow *et al.*, 1998).

| | **Uniform temperature** | | **Uniform heat flux** | |
|---|---|---|---|---|
| $D_{io}/D_{oi}$ | $Nu_i$ | $Nu_o$ | $Nu_i$ | $Nu_o$ |
| 0.02 | 32.34 | 3.65 | 32.71 | 4.73 |
| 0.05 | 17.46 | 4.06 | 17.81 | 4.79 |
| 0.10 | 11.56 | 4.11 | 11.91 | 4.83 |
| 0.25 | 7.37 | 4.23 | 7.75 | 4.90 |
| 0.50 | 5.74 | 4.43 | 6.18 | 5.03 |

The water properties and the convective heat transfer coefficient remain approximately constant at the heat exchangers but the same affirmation can not be made for R744 parameters, especially at the gas cooler. Therefore, each heat exchanger was divided into many control volumes in this study. The heat transfer rate in each volume is given by Eq. 12:

$$\Delta\dot{Q} = \dot{m}_w c_w \Delta T_w = \dot{m}_r \Delta i \tag{12}$$

The length of each volume was calculated using the Log Mean Temperature Difference method described by Eq. 13 and 14 (Bergman *et al.*, 2011) :

$$UA = \frac{\Delta\dot{Q}}{(\Delta T_{in} - \Delta T_{out})/ln(\Delta T_{in}/\Delta T_{out})} \tag{13}$$

$$\Delta L = UA\left(\frac{1}{h_r \pi D_{ii}} + \frac{ln(D_{oi}/D_{ii})}{2\pi k_{cu}} + \frac{1}{h_w \pi D_{oi}}\right) \tag{14}$$

where $D_{ii}$, $k_{cu}$, $\Delta T_{in}$, $\Delta T_{out}$ are the inner diameter of the inner tube, the copper thermal conductivity, the temperature between water and R744 at the inlet of the control volume, and the temperature between water and R744 at the outlet of the control volume. The heat transfer coefficient ($h_w$) of R744 is calculated using the correlation proposed by Shah (2017) at the boiling region. For turbulent flow, Wang *et al.* (2017) was used in the gas cooler, and Gnielinski (1976) and Zigrang and Sylvester (1982) for super-heated vapor flow at the evaporator. For laminar flow, Cengel *et al.* (2011) recommend Nu=4.36. The correlation of Wang *et al.* (2017), developed with experimental data of R744 flowing in a helical heat exchanger and in the supercritical state, is given by Eq. 15:

$$Nu = 0.022986 Re^{0.85665} Pr^{0.26322}\left(\frac{\rho_p}{\rho_f}\right)^{0.04988}\left(\frac{\bar{c}}{c}\right)^{-0.2174} \tag{15}$$

$$\bar{c} = \frac{i_p - i_f}{T_p - T_f} \tag{16}$$

where the subscript *p* indicates the wall properties. Shah (2017) presented correlations based on 4852 experimental data points from 81 sources and 30 different fluids including R744. The boiling heat transfer coefficient is the largest value given by the Eq. 17. In equation 17, $h_L$ is the liquid heat transfer coefficient calculated using Dittus and Boelter (1930) equation (Eq. 23) , the Froud number is calculated using Eq. 21, the convection number employing Eq. 24, the Weber number using Eq. 25, and the Boiling number applying Eq. 26.

$$h = \text{MAX} \begin{cases} 1.8B_1^{-0.8}B_3h_L \\ 230Bo^{0.5}B_3h_L \\ B_2Bo^{0.5}\text{exp}(2.74B_1^{-0.1})B_3h_L \\ B_2Bo^{0.5}\text{exp}(2.74B_1^{-0.15})B_3h_L \end{cases} \tag{17}$$

$$B_1 = \begin{cases} Co \quad \text{if horizontal with } Fr_L \geq 0.04 \text{ or vertical} \\ 0.38CoFr_L^{-0.3} \quad \text{if horizontal with } Fr_L < 0.04 \end{cases} \tag{18}$$

$$B_2 = \begin{cases} 14.7 \quad Bo \geq 0.0011 \\ 15.4 \quad Bo < 0.0011 \end{cases} \tag{19}$$

$$B_3 = \begin{cases} 2.1 - 0.008We_V - 110Bo \quad B_3 \geq 1 \\ 1 \quad B_3 < 1 \quad \text{or} \quad Fr_L < 0.01 \end{cases} \tag{20}$$

$$Fr_L = \frac{G^2}{\rho_L^2 g D_{ii}} \tag{21}$$

$$G = \frac{4\dot{m}}{\pi D_{ii}^2} \tag{22}$$

$$Nu = 0.023Re^{0.8}Pr^{0.4} \tag{23}$$

$$Co = \left(\frac{1-x}{x}\right)^{0.8}\left(\frac{\rho_V}{\rho_L}\right)^{0.5} \tag{24}$$

$$We_V = \frac{G^2 D_{ii}}{\rho_V \sigma} \tag{25}$$

$$Bo = \frac{q}{Gi_{LV}} \tag{26}$$

In these equations $x$, $g$, $G$, $\sigma$, $q$ are vapor quality, gravity, mass flux, surface tension and heat flux. Subscripts $V$ and $L$ indicate vapor and liquid properties. To evaluate the mass present in each control volume where there is two-phase flow, it was used Eq. 27 (Humia *et al.*, 2021):

$$\Delta m = \frac{\Delta L \pi D_{ii}^2}{4}(\rho_V \alpha + (1-\alpha)\rho_L) \tag{27}$$

where $\alpha$ is the void fraction that is calculated using the correlation of Hughmark (1962), Eq. 29. The values of $B_1$ are shown in TAB. 2 in function of $B_2$ calculated by Eq. 30. $\alpha_{hom}$ is the void fraction calculated using homogeneous model. The equations for single-phase flow can be obtained from Eq. 27 if $\alpha = 0$ for liquid and $\alpha = 1$ for vapor.

$$\alpha_{hom} = \left[1 + \left(\frac{1-x}{x}\right)\left(\frac{\rho_V}{\rho_L}\right)\right]^{-1} \tag{28}$$

$$\alpha = B_1 \alpha_{hom} \tag{29}$$

$$B_2 = \left[\frac{D_i G}{\mu_L + \alpha(\mu_V - \mu_L)}\right]^{1/6}\left\{\frac{1}{gD_i}\left[\frac{Gx}{\rho_V \alpha_{hom}(1-\alpha_{hom})}\right]^2\right\}^{1/8} \tag{30}$$

Table 2. Parameters of Hughmark's correlation (Duarte, 2018)

| $B_2$ | $B_1$ | $B_2$ | $B_1$ |
|---|---|---|---|
| 1.3 | 0.185 | 8.0 | 0.767 |
| 1.5 | 0.228 | 10 | 0.780 |
| 2.0 | 0.325 | 15 | 0.808 |
| 3.0 | 0.490 | 20 | 0.830 |
| 4.0 | 0.605 | 40 | 0.880 |
| 5.0 | 0.675 | 70 | 0.930 |
| 6.0 | 0.720 | 130 | 0.980 |

And COP is given by:

$$COP = \frac{\dot{Q}_e}{\dot{W}} \tag{31}$$

To evaluate the capillary tube length it was used the correlation (Eq. 32) proposed by Rocha *et al.* (2019) for R744. In equation 32, $P_{sat}$ is the saturation pressure at the isenthalpic line of the expansion process. The parameters used in this work are listed in Tab. 3. The cooper properties in Tab. 3 were obtained from Cengel *et al.* (2011).

$$\pi_a = \pi_b^{-0.4152} \pi_c^{0.0961} \pi_d^{-0.5450} \pi_e^{-0.1601} \tag{32}$$

$$\pi_a = \frac{1.273\dot{m}}{D^2\sqrt{P_{in}\rho_{in}}} \tag{33}$$

$$\pi_b = \frac{P_{sat}}{P_{in}} \tag{34}$$

$$\pi_c = \frac{\rho_V}{\rho_L} \tag{35}$$

$$\pi_d = \frac{L}{D} \tag{36}$$

$$\pi_e = \frac{D\sqrt{P_{in}\rho_{in}}}{\mu_{in}} \tag{37}$$

Table 3. Main design parameters

| Parameter | Value | Parameter | Value |
|---|---|---|---|
| Atmospheric Pressure | 101.3 kPa | Inner tube inner diameter | 4.76mm |
| Water inlet temperature | 25$^o$C | Inner tube outer diameter | 6.34mm |
| Water temperature at gas cooler outlet | 45$^o$C | Outer tube inner diameter | 20.8mm |
| Water temperature at evaporator outlet | 5$^o$C | Superheating | 10$^o$C |
| Heat exchanger pinch | 10$^o$C | Copper conductivity | 401W/(mK) |
| Gravitational acceleration | 9.8m/s$^2$ | Copper rugosity | 1.5$\mu$m |
| Internal volume of oil separator | 0.691L | Compressor speed | 3500rpm |
| Internal volume of liquid separator | 1.35L | Compressor swept volume | 1.75cm$^3$ |
| Tube length between expansion valve and gas cooler | 2.2m | Compressor overall efficiency | 29% |
| Tube length between compressor and evaporator | 2.85m | Compressor polytropic index | 1.35 |
| Tube length between compressor and gas cooler | 1.4m | Compressor volumetric efficiency | 75% |
| Tube length between expansion valve and evaporator | 2.4m | Capillary tube diameter | 0.91mm |

## 3. RESULTS

The procedure and equations presented in the previous section were utilized in the development of a calculation routine. This routine was employed to evaluate the influence of the water temperature at the outlet of the evaporator and the temperature difference on the system performance and component size. The first step was to verify the number of divisions required to design the heat exchangers using the guidelines discussed by Eca *et al.* (2022). Table 4 shows the influence of the number of divisions in the length of the heat exchangers and the mass of R744 considering the parameters of Tab. 3. The number of divisions used to determine the heat transfer rate in each heat exchanger has an important role in the length of the gas cooler. An underestimated number of divisions can lead to considerable errors in the total length of the gas cooler, as can be seen in Table 4. As a consequence, any change in the length of the heat exchangers will also produce variations in the total mass of R744. Above 500 divisions there is no significant variation in the length of the heat exchangers when considering three significant figures. In the present study, the maximum difference betwen the results for 500 and 1000 divisions was 0.11%. For the set of parameters obtained with 500 divisions and considering the parameters of Tab. 3, a capillary tube length of 3.17m, a gas cooler pressure of 89 bar, a cooling capacity of 855W, and a COP of 1.16 were obtained.

Figure 2 depicts the influence of these parameters on the capillary tube length. Increasing the $\Delta T_{hx}$ promotes a decrease of the evaporating temperature, or evaporating pressure, and also increases the pressure in the gas cooler as shown in Figure 2b. As the pressure difference between the gas cooler and the evaporator increases, a large capillary

Table 4. Effect of the number of divisions in the length of the heat exchangers and in the total mass of R744

| | 15 | 30 | 60 | 120 | 250 | 500 | 1000 |
|---|---|---|---|---|---|---|---|
| $L_{gc}$ (m) | 23.1 | 21.7 | 21.1 | 20.8 | 20.7 | 20.6 | 20.6 |
| $L_e$ (m) | 12.9 | 13.0 | 12.9 | 12.9 | 12.9 | 12.9 | 12.9 |
| $m$ (g) | 488 | 473 | 467 | 464 | 462 | 462 | 462 |

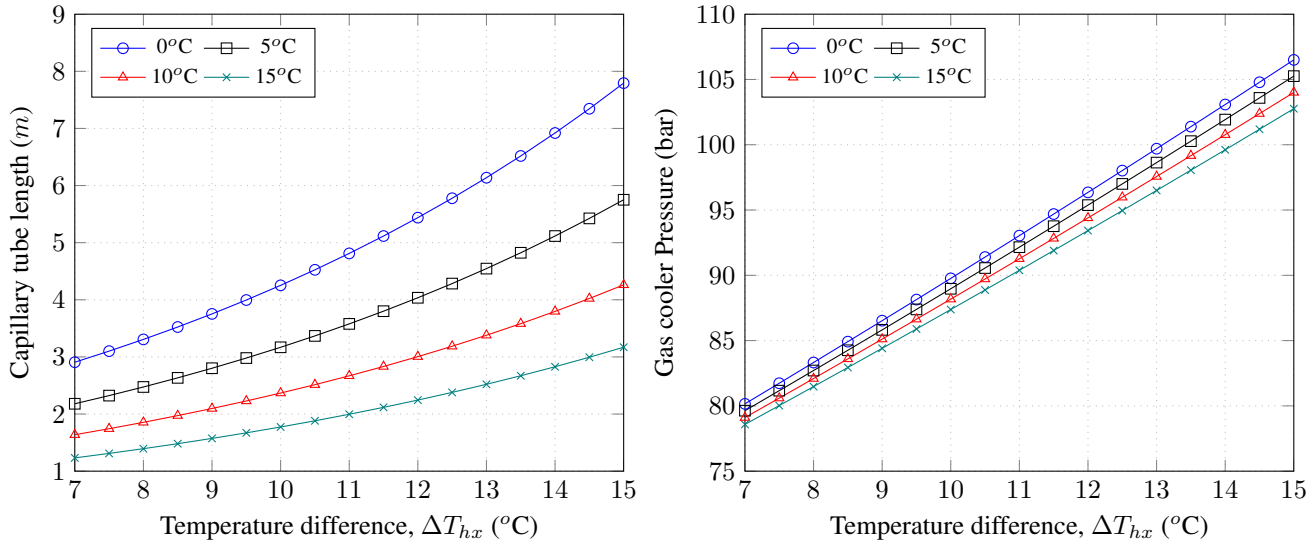


Figure 2. Variation of capillary length (a) and gas cooler pressure (b) in the function of heat exchanger pinch for different water temperatures at the evaporator outlet.

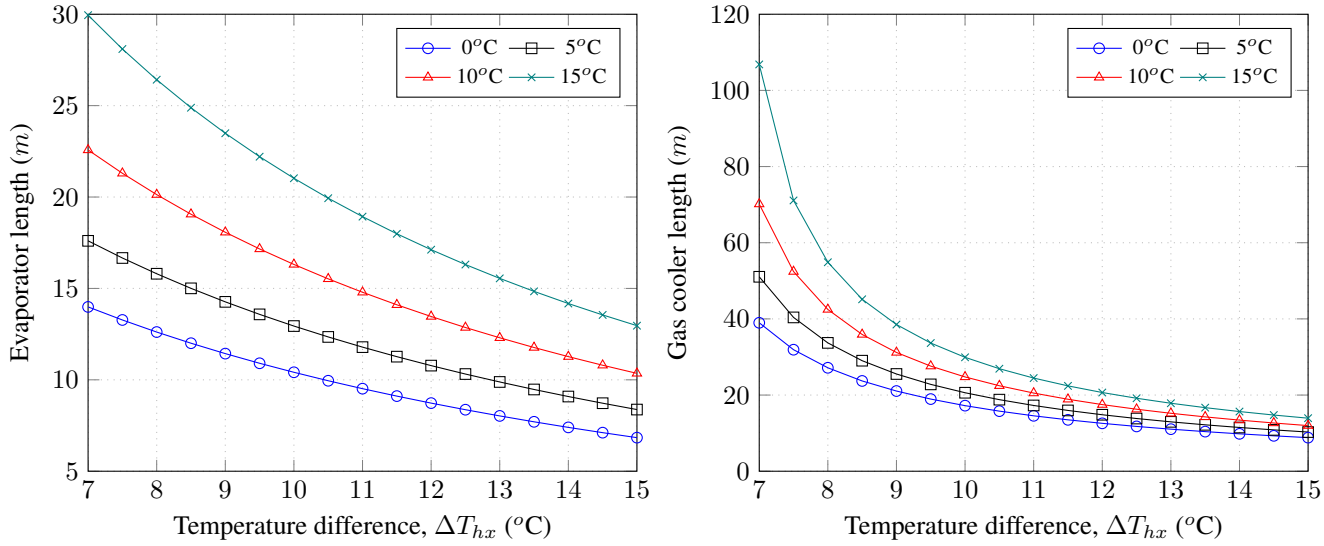


Figure 3. Variation of evaporator length (a) and gas cooler length (b) as a function of heat exchanger pinch for different evaporator water temperature outlet.

tube is required because the pressure loss due to friction in a tube is directly proportional to its length. For the same temperature difference, the capillary tube length increases as the evaporating temperature decreases for the same reason mentioned above.

Figure 3 shows the influence of the $\Delta T_{hx}$ and water temperatures at the evaporator outlet on the evaporator (a) and gas cooler (b) lengths. The decrease of the evaporator length with the increase of $\Delta T_{hx}$ is related to the behavior of the cooling capacity with respect to $\Delta T_{ml}$ shown in Fig. 4 (a) and (b). Either the cooling capacity decreases with the increase of $\Delta T_{hx}$ or the increase of $\Delta T_{ml}$ , since the increase of $\Delta T_{hx}$ contributes to the decrease of $UA$ value. Since the convective heat transfer coefficient remains approximately constant the area and the length are reduced. The contrary effect is observed by increasing the water temperatures at the evaporator outlet, increasing the cooling capacity, decreasing the $\Delta T_{ml}$, and increasing the evaporator length. Similar behavior is observed for the gas cooler length for the same reasons.

Figure 5 presents the mass (a) and the COP (b) for different outlet water temperatures and $\Delta T_{hx}$. The mass variation is related to the length of the heat exchangers. Since the augment of $\Delta T_{hx}$ and the outlet water temperature increases the length of the evaporator and the gas cooler, it will also increase the total mass of R744. The variation of COP is justified due to the increase in the $\Delta T_{hx}$ that promotes a decrease of the evaporating temperature and also increases a gas cooler pressure as shown Fig. 2, both phenomena contributed contribute to the decrease of the COP.

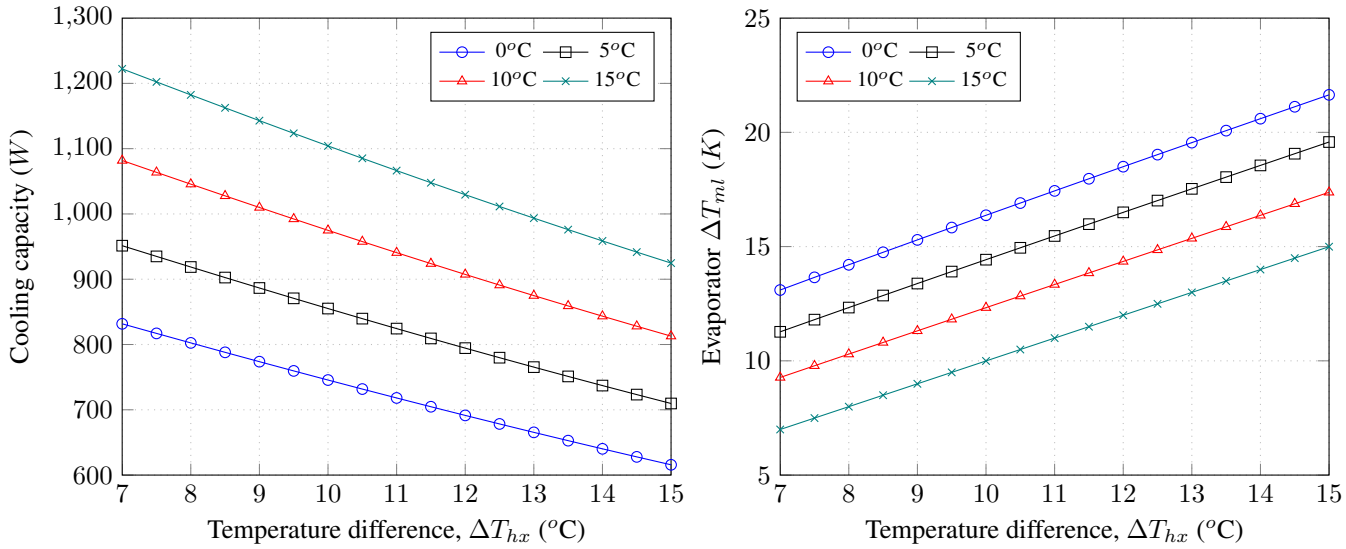


Figure 4. Variation of the cooling capacity (a) and Evaporator $\Delta T_{ml}$ (b) as a function of heat exchanger pinch for different water temperatures at the outlet of the evaporator.

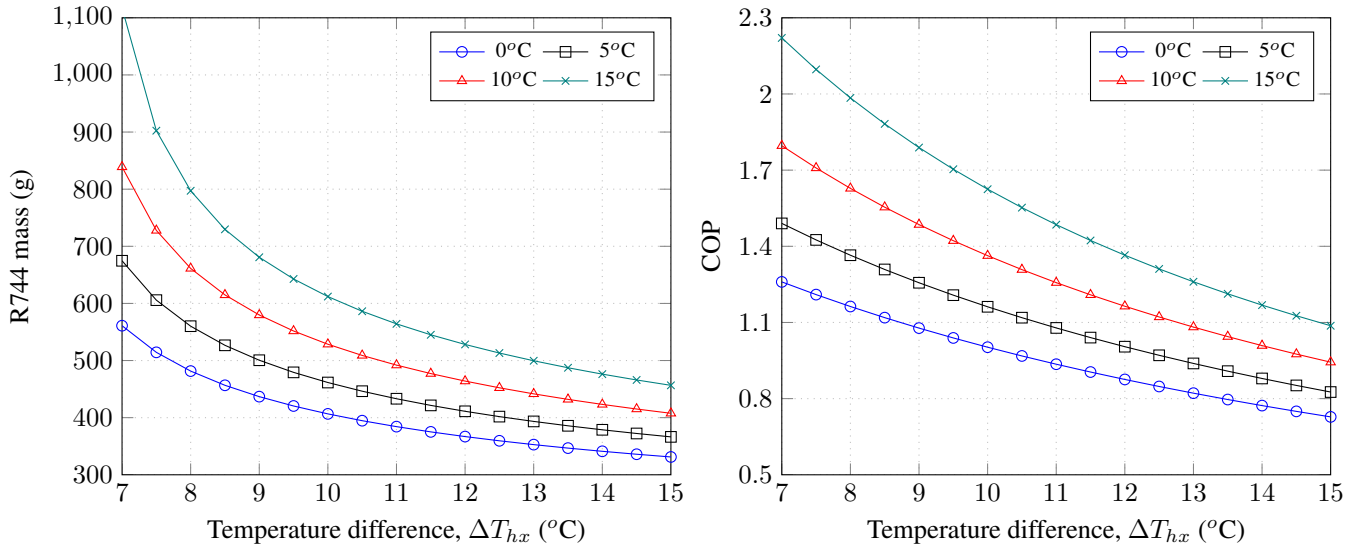


Figure 5. Variation of R744 mass (a) and COP (b) regarding the heat exchanger pinch for different water temperatures at the evaporator outlet.

## 4. CONCLUSIONS

In this work, a methodology for the design of a refrigeration system operating with R744 has been presented. From the proposed design methodology, a computer routine was developed to perform all calculations. This routine was employed to generate a series of curves covering different operating points, which allowed understanding the impact of some parameters in the component size and on the system COP. In the end, the computer routine was used to design a small-capacity refrigeration system operating with R744. The system was designed to operate with an evaporator of 12.9m, a gas cooler of 20.6m, a capillary tube of 3.17m, and a charge of R744 of 462g. The set of curves can be used to match the operational requisites with the specifications of the parts available on the market.

## 5. SUPPLEMENTARY MATERIAL

A Python script used in the work can be found online at
https://colab.research.google.com/drive/1RTzrL8FSly4OGo2ZYwbZTSsWS3jKDCGs?usp=sharing

## 6. ACKNOWLEDGEMENTS

This work was supported by the Foundation for Research Support of the State of Minas Gerais (FAPEMIG), the National Council for Scientific and Technological Development (CNPq), and the Coordination of Improvement of Higher Level Personnel (CAPES).

## 7. REFERENCES

Bell, I.H., Wronski, J., Quoilin, S. and Lemort, V., 2014. "Pure and pseudo-pure fluid thermophysical property evaluation and the open-source thermophysical property library coolprop". *Industrial & Engineering Chemistry Research*, Vol. 53, No. 6, pp. 2498–2508. doi:10.1021/ie4033999.

Bergman, T.L., Lavine, A.S., Incropera, F.P. and DeWitt, D.P., 2011. *Introduction to heat transfer*. John Wiley & Sons.

Cabeza, L.F., de Gracia, A., Fernández, A.I. and Farid, M.M., 2017. "Supercritical co2 as heat transfer fluid: A review". *Applied thermal engineering*, Vol. 125, pp. 799–810.

Cengel, Y.A., Ghajar, A.J. and Kanoglu, M., 2011. "Heat and mass transfer: fundamentals and applications".

de Freitas Paulino, T., de Oliveira, R.N., Maia, A.A.T., Palm, B. and Machado, L., 2019. "Modeling and experimental analysis of the solar radiation in a co2 direct-expansion solar-assisted heat pump". *Applied Thermal Engineering*, Vol. 148, pp. 160–172.

de Paula, C.H., Duarte, W.M., Rocha, T.T.M., de Oliveira, R.N., de Paoli Mendes, R. and Maia, A.A.T., 2020a. "Thermo-economic and environmental analysis of a small capacity vapor compression refrigeration system using R290, R1234yf, and R600a". *International Journal of Refrigeration*, Vol. 118, pp. 250–260.

de Paula, C.H., Duarte, W.M., Rocha, T.T.M., de Oliveira, R.N. and Maia, A.A.T., 2020b. "Optimal design and environmental, energy and exergy analysis of a vapor compression refrigeration system using R290, R1234yf, and R744 as alternatives to replace r134a". *International Journal of Refrigeration*, Vol. 113, pp. 10–20.

de Paula, Y.F., 2022. *Projeto de uma bancada de refrigeração utilizando o R744 como fluido refrigerante*. Bachelor's thesis, UFMG, Belo Horizonte, MG, Brazil.

Dittus, F. and Boelter, L., 1930. "Heat transfer in automobile radiators of the tubular type". *University of California Engineering Publication 13:443*.

Duarte, W.M., 2018. *Numeric model of a direct expansion solar assisted heat pump water heater operating with low GWP refrigerants (R1234yf, R290, R600a and R744) for replacement of R134a*. Ph.D. thesis, UFMG.

Eca, L., Dowding, K. and Roache, P.J., 2022. "On the interpretation and scope of the v&v 20 standard for verification and validation in computational fluid dynamics and heat transfer". *Journal of Verification, Validation and Uncertainty Quantification*, Vol. 7, No. 2, p. 021005.

Gnielinski, V., 1976. "New equations for heat and mass transfer in turbulent pipe and channel flow". *Int. Chem. Eng.*, Vol. 16, No. 2, pp. 359–368.

Hughmark, G., 1962. "Holdup in gas liquid flow". *Chemical Engineering Progress*, , No. 58, pp. 62–65.

Humia, G.M., 2022. *Estudo experimental e modelo de simulação do inventário de refrigerante em uma bomba de calor a CO2 dotada de evaporador solar*. Ph.D. thesis, UFMG.

Humia, G.M., Duarte, W.M., Pabon, J.J.G., de Freitas Paulino, T. and Machado, L., 2021. "Experimental study and simulation model of a direct expansion solar assisted heat pump to co2 for water heating: Inventory, coefficient of performance and total equivalent warming impact". *Solar Energy*, Vol. 230, pp. 278–297.

Maia, A., Koury, R. and Machado, L., 2013. "Development of a control algorithm employing data generated by a white box mathematical model". *Applied thermal engineering*, Vol. 54, No. 1, pp. 120–130.

Rabelo, S.N., Paulino, T.F., Machado, L. and Duarte, W.M., 2019. "Economic analysis and design optimization of a direct expansion solar assisted heat pump". *Solar Energy*, Vol. 188, pp. 164–174.

Rocha, T., Campos, F., Faria, V.S., Paulino, T.d.F. and Nunes, R., 2019. "Assessment of different methods for predicting the mass flow rate through adiabatic capillary tubes". In *25th International Congress of Mechanical Engineering—COBEM 2019*.

Rohsenow, W.M., Hartnett, J.P., Cho, Y.I. *et al.*, 1998. *Handbook of heat transfer*, Vol. 3. McGraw-Hill.

Shah, M.M., 2017. "Unified correlation for heat transfer during boiling in plain mini/micro and conventional channels". *International journal of refrigeration*, Vol. 74, pp. 606–626.

Wang, K.Z., Xu, X.X., Liu, C., Bai, W.J. and Dang, C.b., 2017. "Experimental and numerical investigation on heat transfer characteristics of supercritical co2 in the cooled helically coiled tube". *International journal of heat and mass transfer*, Vol. 108, pp. 1645–1655.

Yang, L., Li, H., Cai, S.W., Shao, L.L. and Zhang, C.L., 2015. "Minimizing cop loss from optimal high pressure correlation for transcritical co 2 cycle". *Applied Thermal Engineering*, Vol. 89, pp. 656–662.

Zigrang, D. and Sylvester, N., 1982. "Explicit approximations to the solution of colebrook's friction factor equation". *AIChE Journal*, Vol. 28, No. 3, pp. 514–515.

## 8. RESPONSIBILITY NOTICE

The authors are solely responsible for the printed material included in this paper.